Proceedings of ISFOG 2025
5TH INTERNATIONAL SYMPOSIUM ON
FRONTIERS IN OFFSHORE GEOTECHNICS
Nantes, France | June 9-13 2025

ISBN 978-2-85782-758-0

Geohazard evaluations on clay-rich submarine landslides combining experimental and numerical methods

E. R. Sørlie*[1,3], Q.A. Tran[1], S.A. Degago[1,2], G.R. Eiksund[1], T. Thomassen[2]
[1]*Norwegian University of Technology, Trondheim, Norway*
[2]*Norwegian Public Road Administration, Oslo, Norway*
[3]*Multiconsult Norge AS, Oslo, Norway*
**erik.sorlie@ntnu.no (corresponding author)*

ABSTRACT: This paper highlights the research on submarine landslides conducted in conjunction with the Norwegian Public Roads Administration (NPRA) mega-project "Ferry Free E39" from Kristiansand to Trondheim, where the long-term goal is to replace the ferry crossings with bridges and tunnels along the costal highway in the western part of Norway. The research presented herein combines physical model testing and numerical simulations and have been tailored to the Bjørnafjorden crossing. The experimental studies have focused on different aspects of submarine landslides, including possible impact with offshore foundations and seabed entrainment. These experiments have further been used for validation of numerical simulations. The numerical simulations were performed with the recently developed material point method coupled with computational fluid dynamics (MPM-CFD method). This method has also been successfully adopted to simulate a previous identified submarine landslide at Bjørnafjorden. In both conditions, the simulations were determined from detailed geotechnical soil tests. Finally, this paper shows how the combined experimental and numerical analyses can be used to quantify the impact forces and the integrity on seabed foundations. This integrated study outlines a general methodology that can be used to quantify the geohazard related risk for similar future projects.

Keywords: Submarine landslides, Physical model testing, Coupled MPM-CFD, Integrated risk studies.

1 BACKGROUND

The background of the study is the NPRA mega-project Ferry Free E39, with a focus on the Hordfast project (www.hordfast.no). The purpose of the project is to cross the 5 km wide fjord Bjørnafjorden, in the Western part of Norway, with a floating bridge. Geophysical surveys have identified numerous past landslide events in the vicinity of the planned bridge (Solli et al., 2017, NPRA, 2019) while soil investigations and stability evaluations have shown that there are still marginally stable accumulations of soil deposits at the flanks (Carlton et al., 2019). The planned foundation concept for the floating bridge consists of mooring lines attached to suction anchors in the fjord seabed. Thus, future submarine landslides may have potential to impact both the anchors and the mooring lines. Evaluation of the submarine landslides, including possible impact scenarios, is therefore a crucial design condition for the integrity of the bridge.

2 SHORT ON SUBMARINE LANDSLIDES

Submarine landslides present risks to structures and facilities located offshore and near the shore, as they have the potential to generate significant impact forces, entrain the seabed, and potentially trigger tsunamis (Hampton et al, 1996; Locat and Lee, 2002; Harbitz et al., 2004; Puzrin, 2016; Sassa, 2023). Earlier events have led to collapse of offshore platforms, breaking of pipelines and seabed cables as well as catastrophic damage from tsunamis (e.g., Heezen and Ewing, 1952; Bea et al, 1983). Areas prone to submarine landslides include delta areas, fjords, open continental shelves, submarine canyons and at volcanoes (Locat and Lee, 2002). Common triggering factors for submarine landslides include earthquakes, waves loads, rapid sedimentations, artesian pore-pressures, weak layers and human induced activities, as shown in Figure 1. Submarine landslides are commonly studied through combined geophysical and geotechnical surveys to characterize the morphology. Furthermore, the knowledge of submarine landslides has increased from previously conducted experimental studies and numerical studies (e.g., Elverhoi et al, 2010; Sørlie et al. 2023a; 2025).

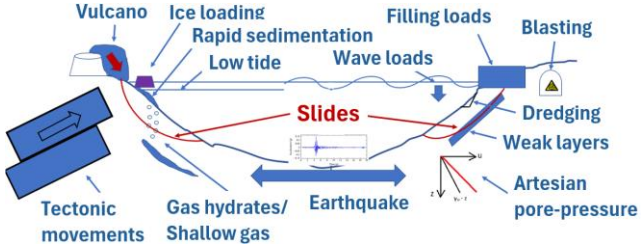

Figure 1. Common triggers of submarine landslides.

3 RESEARCH OUTCOMES OF E39 BJØRNAFJORDEN PROJECT

3.1 Outcomes of geotechnical and geophysical surveys

Geotechnical and geophysical surveys were conducted as part of the Bjørnafjorden bridge crossing project. The geophysical surveys included multi-beam bathymetry (MBE) and sub-bottom profile (SBP) lines with a grid space of 50 m. The landslide mapping identified 45 individual slide events in the fjord. Age dating analyses of selected slide lobes showed that these slide events consisted of minimum 3 triggering events in the last 2000 years (Solli et al., 2017; NPRA 2019). Figure 2 shows the sample locations while Figure 3 shows estimated time of occurrence for of the detected slide events. Subsequent geotechnical investigations have been the basis for a preliminary geohazard study (Carlton et al., 2019) and for the research project presented herein.

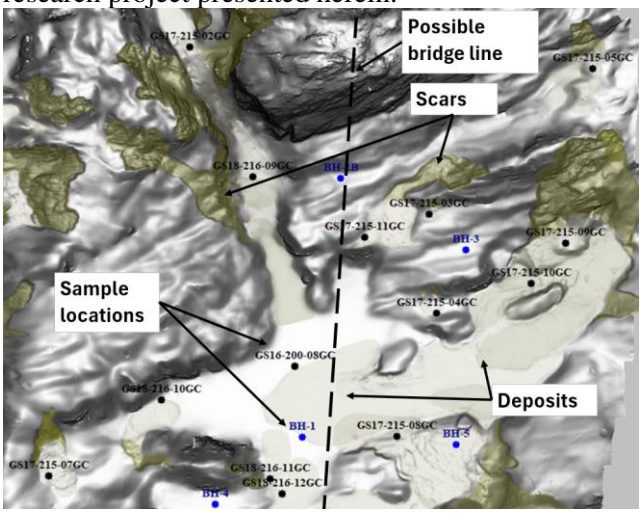

Figure 2. Hill-shade plot of bride area (After NPRA219).

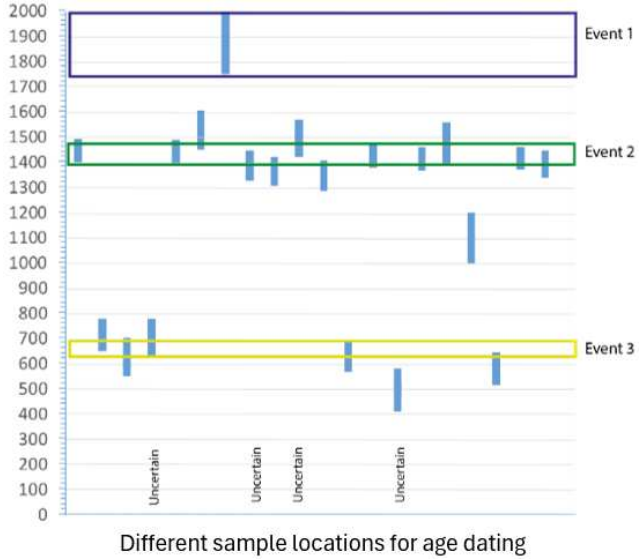

Figure 3. Age dating results; X-axis is sample locations from Fig. 1, Y-axis represent years AD (NPRA, 2019).

3.2 Outcomes of this research project: "Impact loads on offshore foundations"

This present project has combined different research methods, including laboratory testing, physical modelling and numerical simulations as follows:

1. Detailed laboratory tests have been conducted for the soil materials to be used for the physical model testing and on Bjørnafjorden samples.
2. Experiments focusing on submarine impact scenarios have been performed.
3. An advanced continuum modelling approach capable of simulating both model test scales and field scales have been validated.
4. The continuum modelling approach and the outcomes of the physical model testing is combined for foundation integrity evaluations, as shown in this paper.

The soil material used for the physical model testing is mixtures of kaolin clay. The rheological behaviour of kaolin clay and Bjørnafjorden clay were investigated in laboratory tests. The strain rate dependency was measured using cyclic direct simple shear (DSS) tests, T-bar tests and viscometer tests. The normalized results for kaolin clay, used for the experiments, are shown in Figure 4. The different testing devices enabled to measure the strain rate dependency covering strain rates between 10^{-2} to 10^{5} %/s. The testing program also included evaluation of the post-cyclic shear strengths from cyclic DSS tests. The results from these tests showed a relationship between the reduction in shear strengths and the permanent excess pore pressure ratio ($\Delta u_p/\sigma_{v0}$'). The performed lab tests were presented in Sørlie et al. (2022; 2023a).

The physical model testing of submarine landslides investigated; (1) the flow velocity vs time, (2) the flow mechanisms and (3) impact with a foundation pillar. Figure 5 shows the flow prior to and after impacting with the pillar, while Figure 6 show a normalized plot of the impact forces. The normalization enables scaling from the model test condition to field scale. The Y-axis is the equivalent drag coefficient of the pillar (eq. 1) while the X-axis is the non-Newtonian Reynolds-number (eq. 2). The experiments were performed with a flume inclination of the run-out section of 12 and 18 degrees. Different water contents of the soil were considered to give a range in the soil properties. The initial soil state was either remoulded or with a one-day of self-weight consolidation. The trendline in Figure 6 was based on a hybrid hydro-dynamic and geotechnical model (eq. 3), with obtained fitted coefficients of $C_{d,hyb.}$=1.06, $N_{p,hyb.}$=5.2. The variables in the equations are the maximum impact force (Q_{max}), the pillar foundation

diameter (D), the flow height prior to pillar impact (H_{flow}), the soil density (ρ_{soil}), the flow head velocity (U), the shear strength of the soil during the impact also accounting for strain rate effects (τ_y), and the impact pressure (q_{impact}). The data from the physical model testing is included in Sørlie et al. (2023a;2024).

$$C_d = \frac{Q_{impact}/(D \cdot H_{flow})}{\frac{1}{2}\rho_{soil} \cdot U^2} = \frac{q_{impact}}{\frac{1}{2}\rho_{soil} \cdot U^2} \quad (1)$$

$$Re_{non-newtonian} = \frac{\rho_{soil} \cdot U^2}{\tau_y} \quad (2)$$

$$q_{impact} = \frac{1}{2} C_{d,hyb.} \cdot \rho_{flow} \cdot U^2 + N_{p,hyb.} \cdot \tau_y \quad (3)$$

The results from the physical model testing were combined with field data from Bjørnafjorden to validate an advanced continuous modelling method. The newly developed coupled MPM-CFD method (Tran et al., 2024a) was used for this purpose. The observed response in both the physical and numerical analyses showed a strong similarity, as presented in Figure 7 to Figure 11. The geotechnical properties were used directly from geotechnical lab testing, thus providing a validation of the MPM-CFD model. See Sørlie et al. (2025) for full details. The model was further applied in Sørlie et al. (2023b) for a possible future slide event at Bjørnafjorden, while more generic cases will be presented in the subsequent section. The MPM-CFD method was further validated on sand-rich submarine landslides in Tran et al. (2024b).

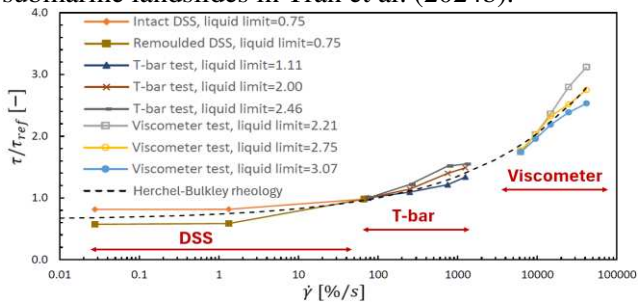

Figure 4. Compilation of soil tests in terms of strain rate effects for kaolin clay (Sørlie et al., 2023a).

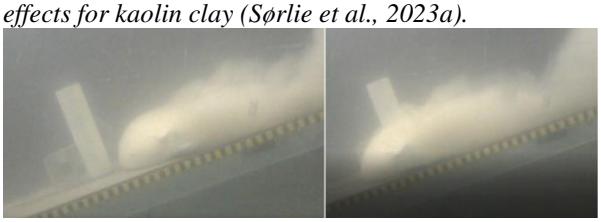

Figure 5. Model test experiment of submarine landslide impacting with a pillar foundation (Sørlie et al. (2023a).

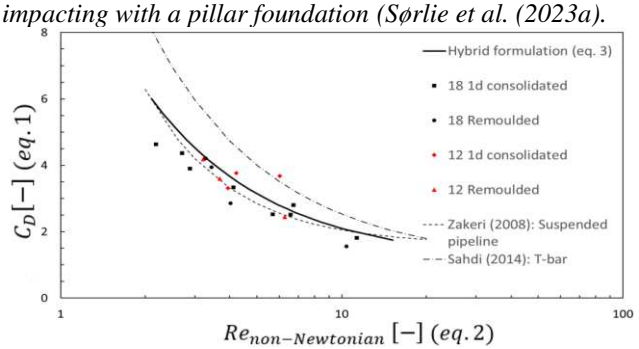

Figure 6. Normalized impact forces on foundation pillar (Sørlie et al. 2023a).

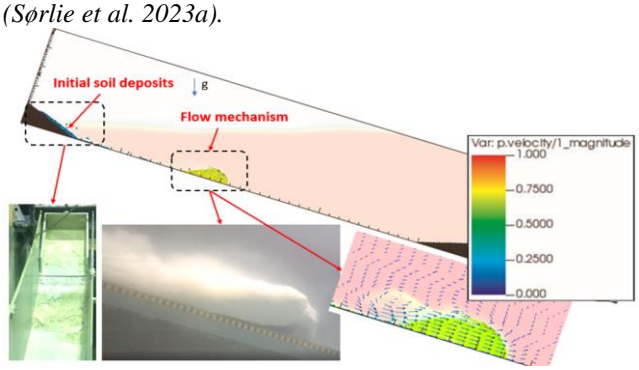

Figure 7. Slide mechanisms from MPM-CFD analysis and observation from the corresponding experiment (Sørlie et al. 2025).

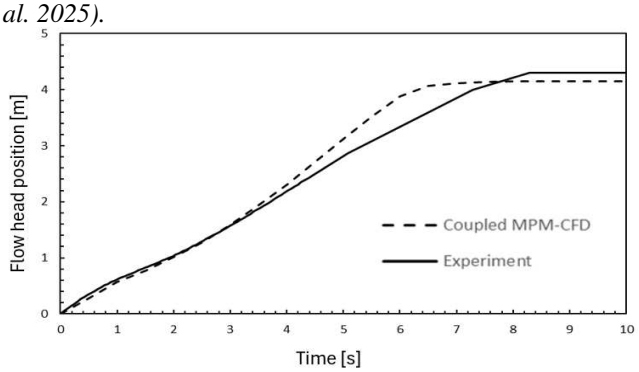

Figure 8.Landslide envelope from MPM-CFD simulation and the corresponding experiment (Sørlie et al. 2025).

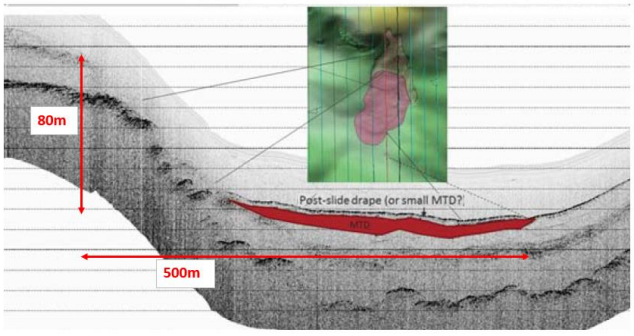

Figure 9. Slide event at Bjørnafjorden from SBP data and hill-shade plot (NPRA, 2019).

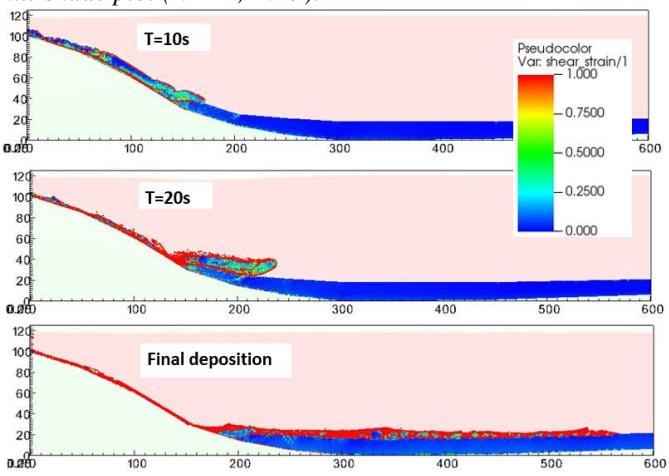

Figure 10. MPM-CFD analyses of Bjørnafjorden slide at different time instances after slide initiation (Sørlie et al. 2025).

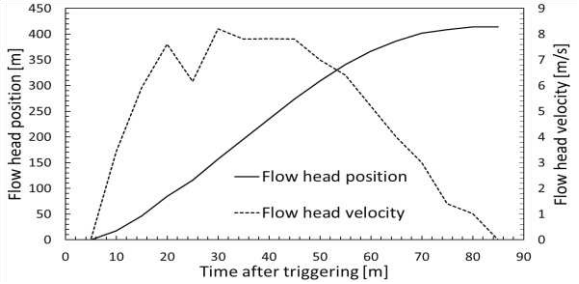

Figure 11. Data from MPM-CFD analyses; Flow head velocity and flow head position vs time (Sørlie et al. 2025).

4 APPLICATION OF MPM-CFD METHOD ON BJØRNAFJORDEN FLANKS

4.1 MPM-CFD analyses of generic flanks

This section presents three coupled MPM-CFD simulations, which resembles typical Bjørnafjorden slopes. These analyses are extension of the MPM-CFD simulation in Sørlie et al. (2023b). The simulations have the same underlying assumptions, except the lengths of the flank, where three flank lengths are considered. The same flank gradient of 1:2.5 is used together with a layer thickness of the flank of 10 m, while the vertical distance between top of flank to the basin is H=40, 80 and 120 m. The geometries are specifically defined to cover the typical identified slide events from the landslide mapping at Bjørnafjorden (Solli et al., 2017; NPRA, 2019). The final deposits in the MPM-CFD simulations are shown for the three cases in Figure 12, while Figure 13 and Figure 14 show the flow head position and velocity versus time after triggering. The key results of the analyses are summarized in Table 1. It is observed that the run-out distance (L), the total change in head position (ΔL) and the flow head velocities (U_{head}) and seabed entrainment increase with increasing lengths of the flanks, while the normalized run-out distance (H/L) slightly decreases. The seabed entrainment in Table 1 is extracted 50 m from the transition between the flank and basin. This value decreased along the fjord basin.

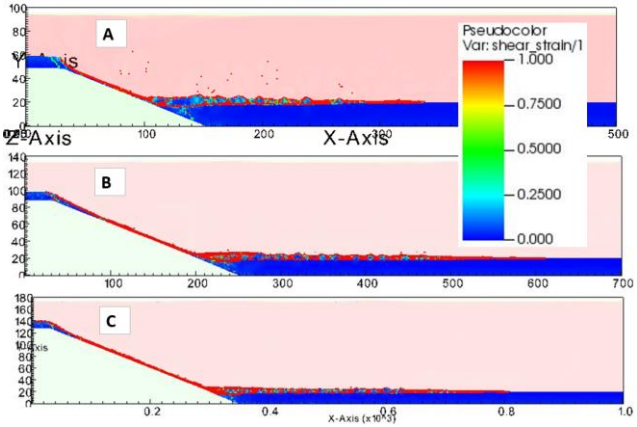

Figure 12. Final slide deposits of MPM-CFD analyses.

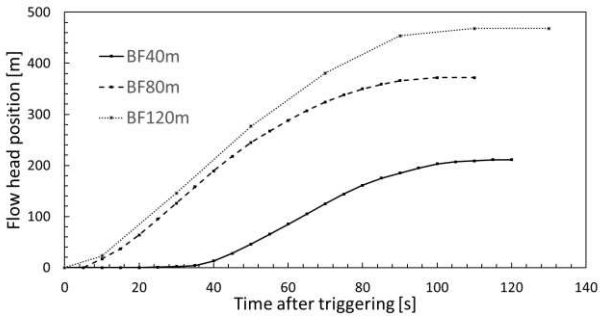

Figure 13. Fow head position vs time.

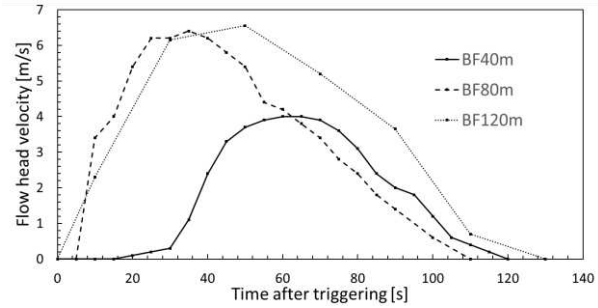

Figure 14. Flow head velocity vs time.

Table 1. Key results MPM-CFD analyses BF flanks

Parameter	BF, H=40m	BF, H=80m	BF, H=120m
L	344m	592m	792m
ΔL	211m	372m	468m
Max U_{head}	4.0m/s	6.3m/s	6.5m/s
L/H	8.6	7.4	6.6
Seabed entrainment	1.5m	2.0m	2.5m

4.2 Conversion to bearing capacity checks assessments on suction anchor foundations

The MPM-CFD analyses in previous section estimated the influence zones and landslide dynamics along the run-out phase of the slide events. The foundation integrity may also be evaluated explicitly with the analysis methodology. This would however require 3D analyses in most cases, which are computationally intensive. The impact loads on the foundations can however still be estimated using the key results from the MPM-CFD analyses, together with the findings from the physical model testing of the submarine landslides, where impact forces on pillar foundations were examined. The key data include the flow velocity, the seabed entrainment, the degree of remoulding of the landslide and the height of the landslide for the foundation locations. Figure 15 illustrates the resisting and driving forces during an impact. The driving forces may be decomposed into two contributions: The direct impact forces from the landslide, and additional lateral pressure on the foundation due to the unbalanced submerged weights on each side of the foundation. The direct impact forces on the foundation may further be divided into two parts; one from the overriding debris on top of the

current seabed, and the impact forces from the entrained soil. These parts are in general different, as the entrained soils may have a different flow velocity and a different degree of remoulding than the overriding debris. In the following calculation example, these two direct impact load contribution parts are assumed similar in terms of velocity and remoulding, where the key results from the flow head is considered. The MPM-CFD analyses showed in general that most of the seabed entrainment occurs at the flow head, while the erosion rate of the seabed is low for the rest of the flow. The impact pressure is calculated using eq. 3, with $C_{d,hyb.}$=1.06, $N_{p,hyb.}$=5.2, which was obtained from the physical model testing of submarine landslides impacting with a foundation pillar. The lateral pressure from the unbalanced submerged weights is calculated as a uniform differential lateral pressure with magnitude of $\Delta p=\gamma' \cdot H_{flow}$. The resisting foundation response may be calculated from a quasi-static FEM analysis or be estimated using simplified calculation approaches (Sørlie 2013; Kay and Palix, 2015; Sørlie et al., 2017).

In the following, the utilization ratio of the foundation is based on the MPM-CFD analysis "BF-80m" and for suction anchor geometries with a diameter of D=10 m and skirt lengths of L=10, 12 and 14 m. The shear strength profile is $s_u=2+2 \cdot z$ (kPa), with a soil sensitivity of $S_t=6$. An initial stick-up length of $\Delta L=1$ m is considered. The simplified calculation approach of Sørlie et al. (2017) is used to determine the bearing capacity of the foundations, given by eq. 4 to eq. 7. The ultimate capacities are relative to decoupling point, which is typically located at an elevation of about 70% of the effective skirt length below the seabed for normally consolidated clays. The variables in eq. 4 to eq. 7 is the lateral, moment and vertical bearing factors (N_p, N_M and N_c), skirt diameter (D) and effective skirt length ($L_{eff}=L-L_{stick-up}-e_r$) combined interaction coefficients (a, b and c) and the soil mobilization (f). Values of N_p=9, N_M=0.2, N_c=8, a=2 b=1 and c=3 is used in this example, which is in line with Sørlie et al. (2017).

$$H_u = N_p \cdot D \cdot L_{eff} \cdot s_{u,ave} \quad (4)$$

$$M_u = N_M \cdot L_{eff} \cdot H_u \quad (5)$$

$$V_u = \alpha \cdot \pi \cdot L_{eff} \cdot D \cdot s_{u,ave} + N_c \frac{\pi}{4} D^2 \cdot s_{u,tip} \quad (6)$$

$$\left(\frac{H}{f \cdot H_u}\right)^a + \left(\frac{M}{f \cdot M_u}\right)^b + \left(\frac{V}{f \cdot V_u}\right)^c = 1 \quad (7)$$

Rate effects of the soil according to the rheological soil tests are considered both when evaluating the impact loads and the foundation resistances. The eccentricities between the resultant of the loads to the decoupling point is considered to calculate the resulting overturning moments, which is further used with eq. 7 to calculate the soil mobilization degree, f (=UR, utilization ratio).

By retrieving the flow velocity and flow height, the state of the soil and entrainment depths for the various locations along the fjord basin, a continuous utilization ratio can be determined for various suction anchor geometries, as shown by Figure 16. The resulting impact forces should be combined with the mooring chain loads; this example does however consider the impact loads only.

These utilization ratios may be used as input to construct risk zones for areas susceptible for submarine landslides. Appropriate foundation locations can be determined, and the required suction anchor geometries may be designed for possible landslide impact scenarios.

The integrity of the mooring chain should also be evaluated. For this, a soil-structure interaction model of the soil, the mooring chain and the landslide is required. The impact pressure on the mooring lines can be determined in a similar way as for the suction anchor foundation. First, by retrieving the key results from an MPM-CFD analysis of the landslide, then by converting the landslide response to impact pressure using one of the outlined methods in Figure 6.

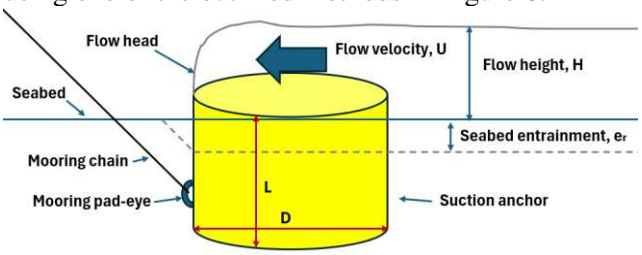

Figure 15. Illustration impact scenario on suction anchor.

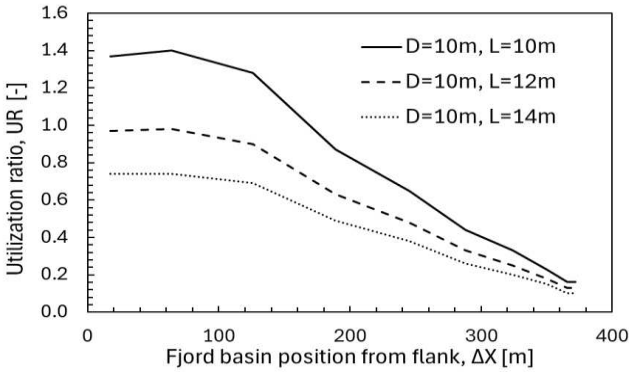

Figure 16. Utilization ratio during impact, case "BF80m" with suction anchor of D=10 m and L= 10, 12 and 14 m.

5 CONCLUSIONS

This paper briefly summarized ongoing research on submarine landslides conducted in connection with the Ferry Free E39 Bjørnafjorden project. Different research methods have been combined, including laboratory testing, experimental studies with physical model, and numerical modelling. The different research activities supplement each other. In short, the

experimental studies have enhanced the understanding of submarine landslide mechanisms, particularly regarding the impact scenario with foundations. The experimental studies have also been the starting point in terms of validating a numerical simulation. A new calculation methodology, the MPM-CFD method, has been developed and validated in terms of both model test condition and from a previous characterised field event. The novel numerical method can investigate all aspects of submarine landslides, from initiation to deposition. Seabed ploughing and the remoulding process from intact soil material to fully remoulded material are explicitly captured in the method. This paper presents how the various research methods can be combined to evaluate the integrity of seabed structures during submarine landslide events. The outcomes can further be used to quantify the geohazards in critical projects and how to mitigate these risks.

AUTHOR CONTRIBUTION STATEMENT

First Author: Methodology, Conceptualization, Data curation, Formal Analysis, Writing- Original draft, Software. **Other Authors**. Software, Supervision, Funding acquisition, Writing- Reviewing and Editing.

ACKNOWLEDGEMENTS

The work has been funded by the Norwegian Public Roads Administration as a part of the Ferry Free 39 Hordfast project. The computations were performed on High Performance Computing resources provided by UNINETT Sigma2 - the National Infrastructure for High Performance Computing and Data Storage in Norway.

REFERENCES

Bea, R.G., Wright, S.G., Sicar, P. & Niedoroda, A.W. (1983). Wave-induced slides in South Pass Block 70, Mississippi delta, *J. Geotech. Eng.* 109, 619-644. DOI: 10.1061/(ASCE)0733-9410(1983)109:4(619)

Carlton, B., Vanneste, M., Forsberg, C.F., Knudsen, S., Løvholt, F., Kvalstad, T., Holm, S., Kjennbakken, H., Mazhar, M.A., Degago, S. & Haflidason, H. (2019). Geohazard assessment related to submarine instabilities in Bjørnafjorden, Norway. Subaqueous Mass Movements. Geological Society, London, Special Publications, 477, 549–566. DOI: 10.1144/SP477.39

Elverhoi A, Breien H, Blasio FVD, Harbitz CB, Pagliardi, M (2010). Submarine landslides and the importance of the initial sediment composition for run-out length and final deposit. *Ocean Dyn* 60, 1027-1046. DOI: 10.1007/s10236-010-0317-z

Hampton, M.A., Lee, H.J. & Locat, J. (1996). Submarine Landslides. *Reviews of Geophysics*, 34, 1, 33-59. DOI: 10.1029/95RG03287

Harbitz, C.B., Løvholt, F. & Bungum, H. (2004). Submarine landslide tsunamis: how extreme and how likely. *Nat. Hazards* 72, 1341-1374. DOI 10.1007/s11069-013-0681-3

Heezen B.C. & Ewing, M. (1952) Turbidity currents and submarine slumps, and the 1929 Grand Banks earthquake. *Am. J. Sci.* 250, 849-873. DOI: 10.2475/ajs.250.12.849

Kay, S. & Palix, E. 2015. Caisson capacity in clay: VHM resistance envelope-Part 2: VHM envelope equation and design procedures. Frontiers in Offshore Geotechnics II Gouvernec & Whote (eds). Taylor and Francis Group, London.

Locat, J. & Lee, H.J. (2002). Submarine landslides: advances and challenges. *Can. Geotech. J.* 39, 193-212. DOI: 10.1139/t01-089

NPRA (2019). Geohazard report, Ferry Free E39 – Fjord crossing Bjørnafjorden

Puzrin, A.M. (2016). Simple criteria for ploughing and runout in post-failure evolution of submarine landslides. *Can. Geotech. J.*, Vol. 53, 1305–1314. DOI: 10.1139/cgj-2015-0582

Sassa, S. (2023). Landslides and Tsunamis: Multi Geohazards. *Landslides*, 20,1335–1341. DOI:10.1007/s10346023-02084-w

Solli, K., Vikebø, J.A., Søyland, E., Hjelstuen, B.O., Kjennbakken, H. & Thomassen, T. (2017). Detailed site survey examining the postglacial sediment succession and depositional processes within a Norwegian fjord system, Bjørnafjorden (West Norway). *Nor. J. Geology* 97, 95–104. DOI: 10.17850/njg97-2-02

Sørlie, E. (2013). Bearing capacity failure envelope of suction caissons subjected to combined loading. Trondheim, NTNU.

Sørlie, E. R., Bendzovski, R., Athanasiu, C., Bye, A. and Giese, S. (2017). A modified modal earthquake analysis of caisson foundations, Proceedings of the XVII ECSMGE-2019

Sørlie, E.R., Hartnik, L.O., Tran, Q.A. & Eiksund, G.R. (2022). Rheological parameters for submarine landslide materials. *10th Int. C. of Physical Modelling in Geotech.*, 153-156

Sørlie, E.R., Hartnik, L.O., Tran, Q.A., Eiksund, G.R., Degago, S.A. & Kjennbakken, H. (2023a). Physical model testing of clay-rich submarine landslides and its interaction with offshore foundation. *Ocean Engineering* 273. DOI: 10.1016/j.oceaneng.2023.113966

Sørlie, E.R, Tran, Q.A., Eiksund, G.R. (2023b). Submarine landslide simulations of steep clay-rich slopes using the material point method coupled with computational fluid dynamics. *9th Int. SUT Offshore Site Investigation and Geotech. C.*, At: London, UK

Sørlie, E.R., Tran, Q.A., Eiksund, G.R., Degago, S.A., Kjennbakken, H., & Johansen, T. F. (2024). Experimental study on erosion of clays during rapid flows. *Ocean Engineering*, *312*, DOI: 10.1016/j.oceaneng.2024.119357

Sørlie, E.R, Tran, Q.A., Eiksund, G.R., Degago, S.A. (2025). Validation of the coupled Material Point Method and Computational Fluid Dynamics on clay-rich submarine landslides. *Landslides*. Accepted for publication.

Tran, Q.A., Grimstad, G. & Amiri S.A.G. (2024a). A hybrid MPM-CFD model for simulating coupled problems in porous media. Application to earthquake-induced submarine landslides. *International J. for Num. Methods in Eng.* 125(5), DOI: 10.1002/nme.7383

Tran, Q. A., Sørlie, E., Grimstad, G., Eiksund, G., Takahashi, H., & Sassa, S. (2024b). Influence of sediment permeability in seismic-induced submarine landslide mechanism: CFD-MPM validation with centrifuge tests and analysis. *Com. and Geotech.*, *174*, DOI: 10.1016/j.compgeo.2024.106588.